Chapter 1. Global agroclimatic patterns

Chapter 1 describes the CropWatch agroclimatic indicators—RAIN, TEMP, and RADPAR—along with the agronomic indicator BIOMASS for sixty-two global Crop Production System Zones (CPSZ). A complete list of values is included in Annex A, table A.1. The presented global overview of relatively wet or dry, warm or cold conditions provides the background for subsequent analysis in Chapters 2, 3 and 4. Overall, the current reporting period is characterized by a number of large areas undergoing abnormal conditions.

1.1 Rainfall

Low rainfall, defined as rainfall that is below 70% of the average amount (that is, a negative departure from average in excess of 30%), was recorded in large expanses of land in eastern Asia, affecting northeast China (C38[1]; a departure of -50%), eastern-central Asia (C42, -35%), eastern Siberia (C51, -32%), east Asia (C43, -31%), as well as Taiwan (C42, -41%). In addition to the drought, northeast China (C38), eastern-central Asia (C52) and eastern Siberia (C51) were also affected by above average temperatures, with positive departures larger than 1°C (larger than 2°C in C52), which is significant considering that the average applies to a period of four months and large land areas.

Figure 1.1. Global map of rainfall anomaly (as indicated by the RAIN indicator) for Crop Production System Zones, departure from 13YA, January-April 2014 (percentage)

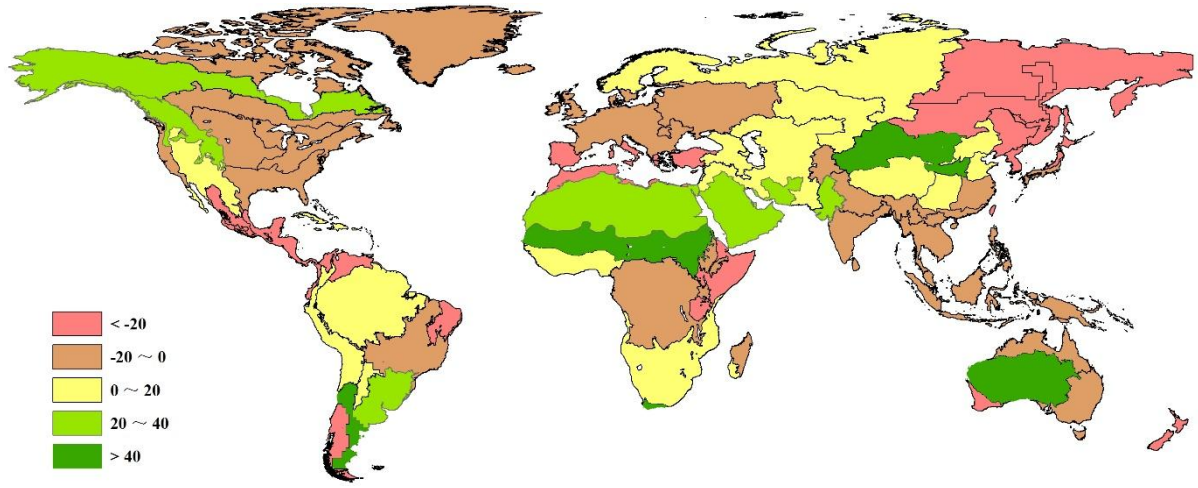

Note: Data for January-April 2014, compared with the thirteen-year average (13YA) for the January-April periods between January 2001 and April 2013.

The following areas all suffered from a rainfall deficit over agricultural areas in excess of 15% (although not all were affected by other unfavorable agroclimatic conditions): New Zealand (C56, -47%), the south-western Southern Cone in Latin America (C27, -46%), Australia from Nullarbor to Darling (C55, -35%), the Brazilian Nordeste (C22, -29%), Sierra Madre in Mexico (C17, -27%), northern South and Central America (C19, -22%), the Horn of Africa (C04, -21%), and -16% in both southern Japan and Korea (C46) as well as in the region from Ukraine to the Ural mountains (C58).

The Mediterranean area is described in two separate zones, which both suffered from rainfall deficits to varying but significant degrees: the North African Mediterranean (C07, -42%), and the European Mediterranean (including Turkey; C59, -26%). The rainfall deficit was accompanied by high temperatures

[1] The Crop Production System Zones (CPSZ) identified by their numbers (e.g., C38) are illustrated in the qick reference guide in this bulletin.

(+1.3°C and +0.6°C, respectively) which resulted in a decreased biomass production potential estimated at -29% in the south and -20% in the north.

Well **above average rainfall** was reported for several areas adjacent to the eastern Asian drought areas, including the China Loess region (C36), Gansu-Xinjiang (C32), and the Mongolia CPSZ (covering approximately the southern half of Mongolia; C47), where the recorded rainfall was about double the recent average.

Other areas worth mentioning include the Sahel (C08, +81%), where high rainfall may point at an early onset of the rainy season in semi-arid West Africa, and several semi-arid or dry areas in the southern hemisphere. They include the Western Cape in South Africa (C10, +44%) as well as several near-deserts and deserts, e.g., the Australian desert CPSZ (C63, +65%) and the semi-arid Southern Cone of Latin America (C28, +44%). The latter observations deserve closer monitoring as they may be linked to El Niño conditions building up (see section 5.2).

Finally, in the area from Punjab to Gujarat at the border of India and Pakistan (C48) rainfall exceeded the recent average by 27%.

1.2 Temperature

Punjab to Gujarat was also one of the regions characterized by **below average temperature** (-1.2°C). Below average temperatures were also recorded for the zone covering central Asia and the Pamir (C30), which borders the Punjab-Gujarat zone to the north and experienced a temperature anomaly of -1.2°C.

Figure 1.2. Global map of air temperature anomaly (as indicated by the TEMP indicator) for Crop Production System Zones, departure from 13YA, January-April 2014 (degrees Celsius)

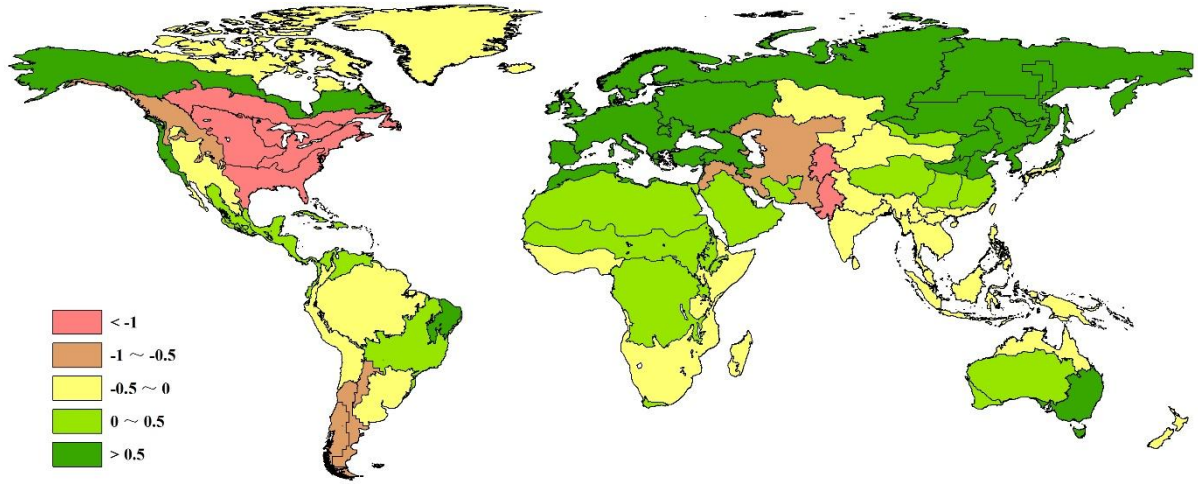

Note: Data for January-April 2014, compared with the thirteen-year average (13YA) for the January-April periods between January 2001 and April 2013.

Record low temperature departures were concentrated in several adjacent areas in North and South America, including (i) the Corn Belt (C13, -2.9°C; the largest departure for any CPSZ), the northern Great Plains (C12, -2.2°C) and the Cotton Belt and Mexican Coastal Plain (C14, -1.7°C); and (ii) the semi-arid Southern Cone (C28) and the south-western Southern Cone (C27), both at -0.8°C. As mentioned above, the semi-arid Southern Cone (C28) also experienced above average rainfall; a similar association between low temperature and high precipitation also applies, to some degree, to the areas mentioned in North America.

Above average temperatures were significant is several areas, although not comparable in intensity to the cold spell that affected most of the main agricultural areas of northern America. Not considering agricultural areas, it is worth noting that the largest positive temperature departures occurred in the northernmost parts of Eurasia and America (boreal Eurasia, +2.2°C in C57; boreal North America, +2.3°C in C61; and eastern Siberia, +1.1 in C51), which is consistent with global warming projections and may eventually, if the "anomalies" become more common, lead to expansion of agriculture into the current permafrost areas.

In areas more relevant for agriculture, the following positive departures are recorded: +1.1°C in northeast China (C38), +1.4°C in China's Huanghuaihai region (C34), and +1.9°C in Inner Mongolia (C35). In the adjacent eastern-central Asia CPSZ the temperature departure was +2.0°C (C52).

Moving closer to Europe, positive temperature anomalies include the relatively low values in the region east of the Black Sea (+1.0°C in the Caucasus CPSZ; C29) and the Ukraine to Ural mountains area (+1.1°C in C58, with a PAR increase of 4%), to reach +1.3°C in Mediterranean Europe and Turkey (C59) and eventually +2.0°C in non-Mediterranean western Europe (C60).

1.3 Photosynthetically active radiation

In several areas in China, the observed **photosynthetically active radiation (PAR)** very consistently followed the rainfall and temperature patterns mentioned above: low rainfall is associated with low cloudiness, which generally leads to high daytime temperatures. The observation applies to the Chinese areas of Gansu-Xinjiang (C32), Huanghuaihai (C34), and the Loess region (C36), which all recorded a 2.0% increase in PAR. The same observation applies to the more southern areas of the island of Hainan (C33) and southwest China (C41). Higher departures (+3%) occurred in the Lower Yangtze region (C37).

Figure 1.3. Global map of PAR anomaly (as indicated by the RADPAR indicator) for Crop Production System Zones, departure from 13YA, January-April 2014 (percentage)

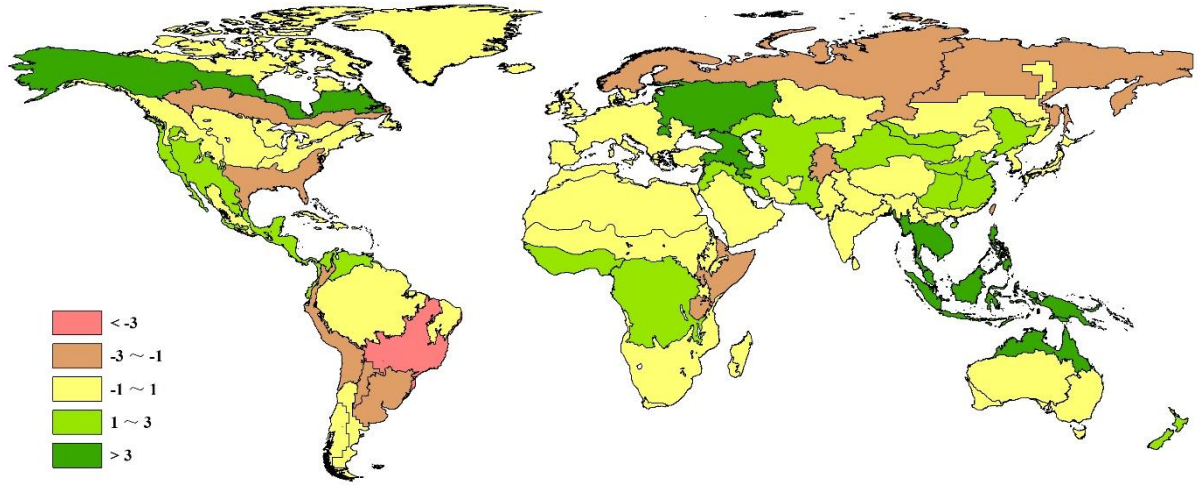

Note: Data for January-April 2014, compared with the thirteen-year average (13YA) for the January-April periods between January 2001 and April 2013.

In other parts of the world, particular mention must be made of the American West Coast (C16, +3% PAR), an area that was also characterized by a positive temperature departure and lower than normal precipitation. Other areas with marked PAR increases are (i) southeast Asia, where both CPSZs (C49, islands; C50, mainland) had a very favorable radiation climate (+3% and +4%, respectively), and (ii) northern Australia (C53, +5%), which neighbors southeast Asia and where observations might be read as an indication of impending El Niño conditions (see section 5.2). The absolute highest PAR departure from

the recent reference period occurred in boreal North America (C61) with +9%. Finally, the area from the Ukraine to the Ural mountains (C58) underwent a PAR increase of 3%.

1.4 Biomass

The potential agricultural impacts from the weather events are synthesized by the **potential biomass estimates.** This CropWatch agronomic indicator is based on both rainfall and temperature and, because of the link between the agroclimatic variables, also linked to radiation.

Figure 1.4. Global map of Biomass accumulation (BIOMASS) for Crop Production System Zones, departure from 13YA, January-April 2014 (percentage)

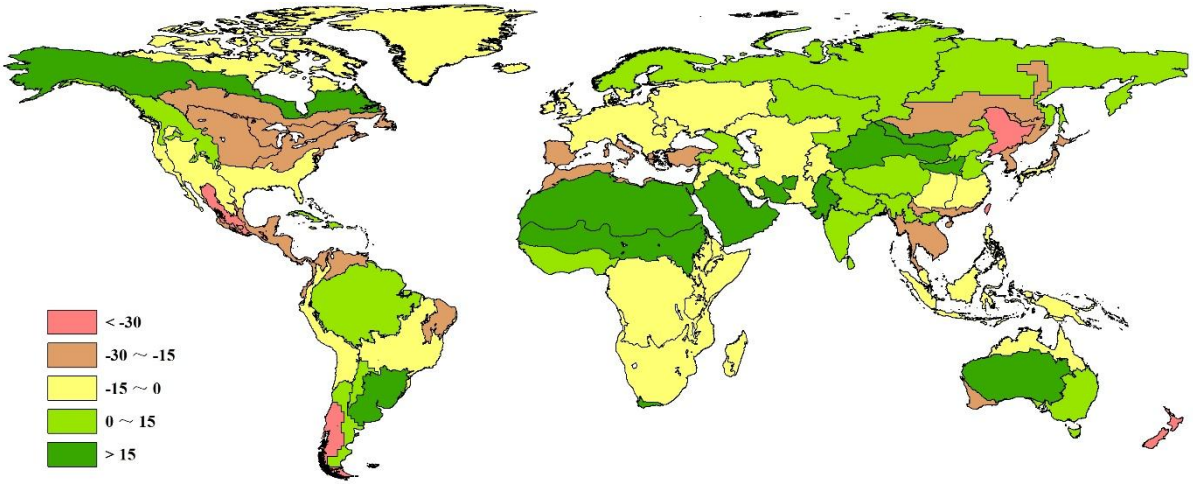

Note: Data for January-April 2014, compared with the thirteen-year average (13YA) for the January-April periods between January 2001 and April 2013.

Particularly poor biomass accumulation conditions prevailed in several parts of Asia, including China (-42% in northeast China, C48; -31% in Taiwan, C42; -29% in southern China, C40; and -17% in Hainan, C33) and adjacent areas (-28% in East Asia, C43; and -24% in eastern-central Asia, C52). A second block of areas with unfavorable conditions for biomass accumulation occurs in North America, with drops in potential biomass in the range of 15 to 20% (corn belt, C13; northwestern Great Plains, C12); and large areas of Mexico and central America (Sierra Madre (C17), -32%; and northern South and Central America (C19), -19%).

Also worth mentioning are negative biomass departures for the two Mediterranean CPSZs (northern Africa (C07), -29%; and Mediterranean Europe and Turkey (C59), -20%), as well as the Brazilian Nordeste (C22, -16%) and the Horn of Africa (-14%, C04).

Some large and very large positive biomass departures are identified in Asia (Gansu-Xinjiang (C32), +68%; Mongolia region (C47), +77%; Punjab to Gujarat (C48), +40%), in Africa ("Sahel" (C08), +72%; western Cape area in South Africa (C10), +33%), and in South America (+19% in some of the major agricultural areas in Brazil and Argentina (C26).